



website: <https://eoge.ut.ac.ir>

Evaluation of sulfur dioxide emissions in thermal power plant and its effect on air quality in the neighboring city using Sentinel-5 images (case study: Iran, Arak)

Mohammad Amin Ghannadi^{1*}, Matin Shahri¹, Saeedeh Alebooye², Amirreza Moradi¹

¹ Department of Surveying Engineering, Arak University of Technology, Arak, Iran

² School of Surveying and Geospatial Engineering, College of Engineering, University of Tehran, Tehran, Iran

Article history:

Received: 15 May 2020, Received in revised form: 25 January 2021, Accepted: 20 February 2021.

ABSTRACT

Sulfur dioxide (SO₂) is one of the most important pollutants in Arak city, and its main source is the Shazand thermal power plant (TPP) which is located along with the dominant southwest wind. This study aims to determine the role of Shazand TPP in the air pollution of Arak. A rational quadratic function is proposed to develop the relationship between SO₂ emitted from Shazand TPP and pollutant concentration in Arak city using Sentinel-5 satellite images over three years. Ground stations for air quality monitoring have also been applied to assess the accuracy of Sentinel-5 satellite observations. The proposed equation was fitted to the Sentinel-5 observations with a precision of 0.15 (relative error). The cross-correlation coefficient between the observations of ground stations for air quality monitoring and Sentinel-5 images is 77%, indicating the reliability of Sentinel-5 satellite data. Experiments demonstrate that the SO₂ density of Shazand TPP can effectively influence the concentration of such pollutant up to 62% in our study area.

KEYWORDS

Air Pollution
Sentinel-5
Sulfur Dioxide
Thermal Power Plant
Google Earth Engine

1. Introduction

Air pollution is increasingly recognized as one of the world's most serious problems, contributing significantly to global climate change and premature death. According to the World Health Organization (WHO), air pollution is the world's leading cause of death, killing about three million people each year (Lelieveld et al., 2015). In many urban areas, the most likely causes of pollution are factors such as population growth, the increase in the number of cars, industrialization and increased energy demand. Therefore, it is essential to reliably assess the amount of air quality at local, regional and global levels with acceptable spatial and

temporal resolution in order to establish the distribution and impact of air pollutants and to provide managers with solutions of various spatial resolutions (Saxena & Naik, 2018). In general, there are several types of pollutants in the atmosphere, the significant consequences of which have become one of the most pressing concerns in the twenty-first century, affecting air quality, the environment, human health, and climate. The most significant air pollutants include sulfur dioxide (SO₂), carbon dioxide (CO₂), carbon monoxide (CO), nitrogen dioxides (NO₂), ozone (O₃), methane (CH₄), unstable organic carbon, chlorofluorocarbons, and suspended particles or aerosols,

* Corresponding author

among which, SO₂ is considered as one of the most toxic gases (Saxena & Naik, 2018).

Coal, petroleum, and other fuels are frequently impure, containing sulfur and various organic chemicals. The sulfur component of fossil fuels produced by burning is the primary anthropogenic source of SO₂ emissions. Sulfur is also emitted in small amounts by forest fires, soil, and plants (Saxena & Naik, 2018). The world's largest SO₂ producer is coal-fired power plants (Tang et al., 2020; Wang et al., 2020), which contributes to pollution, acid rain, and lead to serious health problems such as lung and respiratory diseases (Greenberg et al., 2016).

Emissions, local synoptic weather conditions, topography, and atmospheric chemistry are all contributing factors to air pollution episodes. The relative importance of these elements is determined by various parameters such as emissions, regional and global meteorological conditions, atmospheric chemical processes, geographic region, adjacent source regions, and timing (Kayes et al., 2019; Li et al., 2019; Zeng & Zhang, 2017; Zhang, 2019).

Among various methods of monitoring air pollution, the use of tools and technologies based on remote sensing is especially important because it can generate continuous data in space and time. Due to the low density and non-uniform distribution of ground-based air quality monitoring stations (AQS) in many cities in Iran, the use of satellite remote sensing is useful for monitoring concentrations of air pollutants. In addition, ground-based air pollution monitoring systems have not yet been set up in many Iranian power plants. This allows remote sensing data to be applied to monitor the emissions from power plants.

In remote sensing, information is transmitted by electromagnetic radiation, and vertical profile measurements as well as information about air pollutants (Chen et al., 2018; Lin et al., 2015). The use of satellites and remote sensing to monitor air pollution monitoring provides a suitable platform for global assessment of current air quality and future climate change. Because of factors such as chemical composition, lifetime, and emission sources, accurate monitoring of pollutants is also critical (Saxena & Naik, 2018). Sentinel-5 and its sensor, TROPospheric Monitoring Instrument (TROPOMI), are highly capable of

recording pollution-related data and imaging and tracking various gases and contaminants such as O₃, formaldehyde (HCHO), SO₂, CH₄, CO, aerosols and NO₂.

A review of previous studies indicates the success of applying Sentinel-5 satellite images in monitoring SO₂ (Hedelt et al., 2019; Theys et al., 2019; Wang et al., 2020), CH₄ (Lorente et al., 2021; Schneising et al., 2019) CO (Safarianzengir et al., 2020; Schneising et al., 2019) HCHO (Sun et al., 2021; Vigouroux et al., 2020; Virghileanu et al., 2020), O₃ (Quesada-Ruiz et al., 2020; Zhao et al., 2021), aerosols (Broomandi et al., 2020; Li et al., 2020; Tiwari et al., 2015), NO (Filippini et al., 2020) and NO₂ (Filippini et al., 2020; Ialongo et al., 2020; Koukouli et al., 2021; Omrani et al., 2020; Shikwambana et al., 2020; Virghileanu et al., 2020). The purpose of this article is to model the relationship between SO₂ emitted in Shazand TPP and SO₂ concentrations in Arak using TROPOMI sensor images over a three-year period. The impact of the Shazand power plant on the air quality in Arak will also be assessed. A report on the region's weather situation is also included.

2. Material and Methods

Primarily, the study area is introduced and the data applied is described. The mathematical model of the relationship between SO₂ emissions of TPP and pollutant concentrations in our study area is explained in the next step.

2.1. Study area

In this research, Arak as the capital of Markazi Province and one of the largest metropolitan areas in Iran is studied. Arak is surrounded by mountains on three sides: south, west, and east, with an average altitude of 1750 meters above sea level. It is 260 kilometers distant from Tehran and close to Qom and Isfahan. Arak is 110 square kilometers, and the geographical region of the universal transverse Mercator (UTM) coordinate system extends from the northeast (385500 E, 3777700 N) to the southeast (374600 E, 3769900 N) (Figure 1). Maximum temperature can reach 35° C in summer but can drop below 25° C in the winter. The average annual rainfall is about 350 mm, and the relative humidity is

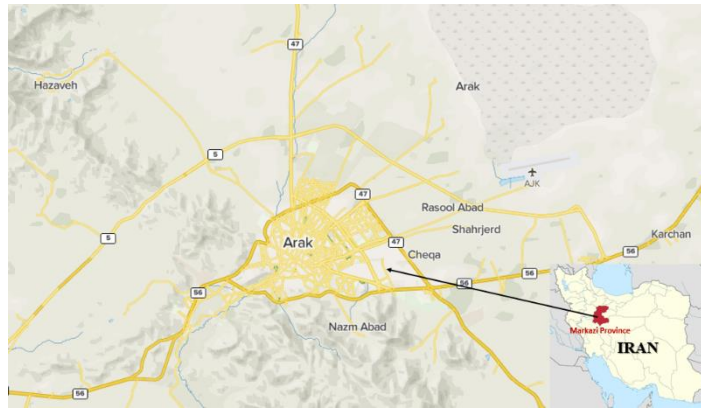


Figure 1. Location of Markazi province and Arak city on the map

46%. In 2016, the population of Arak was estimated to be at 521000, making it the 18th most populous city in Iran. Arak has climatic characteristics similar to those of Iran's central plateau (cold and wet winters and hot and dry summers). The climate of this region is unique, influenced by the mountains surrounding Arak, Meyghan wetland, and the Farahan plain.

Precipitation ranges from 230 to 638 mm depending on the year. Shazand Thermal Power Plant (TPP), Shazand Petrochemical and Refinery, Aluminum, and Machinery manufacturing are Arak's largest industries. Arak ranks first in terms of the diversity of industrial products and second in terms of the presence of basic industries. It is also one of the four industrial hubs of the country. Due to the presence of basic industries, it produces 80% of the country's energy equipment, the existence of the country's largest aluminum producer, the country's largest machine-building industry, the country's largest wagon and locomotive in the Middle East, the Middle East's largest combine, the Middle East's largest producer of heavy machinery and the country's mineral salt firm, Arak is renowned as Iran's industrial hub, making it one of the country's most polluted towns. Not only it is industrial, but it has a relatively high population density (and, therefore, heavy traffic), as well as climate variables that affect its air quality. Claimed to be the main cause of fuel oil burning at Shazand Power Plant and Refinery, SO₂ is arguably one of the most important pollutants in Arak.

2.2. Data

Sentinel-5 is the first satellite of the Copernicus program and one of the most effective in terms of atmospheric monitoring. The TROPOMI sensor on Sentinel-5 can record UV radiation. The number of pollutants included in this research was monitored using TROPOMI level-3 (L3)

products. Sentinel-5 has several important responsibilities, including ensuring data collection from previous (SCIAMACHY, GOME-2, OMI, and Envisat) and future missions (de Vries et al., 2016). TROPOMI collects daily data on the Earth's atmosphere with a spatial resolution of 0.01 arc degrees, which is 13 times better than OMI (Shikwambana et al., 2020). The eight TROPOMI imaging bands include UV, near-infrared (NIR), and short-wave near-infrared (SWNIR) wavelengths (SWIR) (Lorente et al., 2019). TROPOMI can image and monitor many pollutants using three types of processing: NRT (near real-time), OFFL (offline), and reprocessing. Objects for NRT processing must be available within 3 hours of sensing, whereas products for OFFL (Offline) and reprocessing must be available between 12 hours and 5 days after sensing (Shikwambana et al., 2020). One of the most important advantages of Sentinel-5 satellite imaging in pollution monitoring is that it has the ability to collect data at high altitudes in specific areas. This can be useful in determining the geographic distribution of pollutants. However, data collection using Sentinel-5 has limitations such as a small number of observations during the day and the presence of clouds in some observations. Monitoring with such images may not be accurate due to the rapid diffusion of pollutants in the atmosphere.

SO₂ has absorption properties in the infrared band and the initial characteristic wavelengths are 18.9 μm , 8.8 μm and 7.6 μm (Chen et al., 2021). Therefore, TROPOMI can be used to record SO₂ concentrations. In this study, Sentinel-5 images were used to monitor the concentration of SO₂ emitted from Shazand TPP and the concentration of this pollutant in Arak. 1925 images have been recalled on GEE from October 2018 to September 2021. The product used is the vertical column density of SO₂ at the ground level,

calculated using the technique of differential optical absorption spectroscopy (DOAS). The unit of measurement for the concentration of this product is mol/m².

Due to data compatibility reasons, the May-August 2019 SO₂ density monitoring data was not used because the relating meteorological data was not available. GEE data is collected daily by the Copernicus ESA's Sentinel-5 spacecraft (Ghasempour et al., 2021).

Data from AQS were applied to evaluate the accuracy of satellite observations. The cross-correlation coefficient between SO₂ concentrations observed by Arak AQS and TROPOMI sensors will be calculated in 2020.

Iran Meteorological Organization has published some statistics for the Shazand Synoptic Station (ID: 99441), which is located at (Lat: 33.9417°, Lon: 49.4083°). These data include changes in temperature, mean wind speed, mean prevailing wind speed, and prevailing wind direction over the study period. This information contributes to demonstrating the impact of SO₂ emissions from Shazand TPP on air quality in Arak.

2.3. Proposed mathematical model

The steps of the proposed method in this study are shown in the flowchart of Figure 2. In this paper, we investigated the relationship between SO₂ emissions of TPP and SO₂ concentrations in neighboring cities using a rational quadratic function. This is due to the tremendous flexibility of the rational function (Sohn et al., 2005). This equation is suggested as follows:

$$P = \frac{c_0 + c_1 \cdot p + c_2 \cdot p^2}{1 + c_3 \cdot p + c_4 \cdot p^2} \quad (1)$$

P stands for the SO₂ concentration in neighboring cities, while p stands for the SO₂ concentration at the TPP. The

rational equation's coefficients are expressed by the values of c_0 to c_4 , which must be computed.

These equations can also be considered based on equation 1:

$$\begin{bmatrix} P_1 \\ P_2 \\ \cdot \\ \cdot \\ P_n \end{bmatrix} = \begin{bmatrix} 1 & p_1 & p_1^2 & -P_1 \cdot p_1 & -P_1 \cdot p_1^2 \\ 1 & p_2 & p_2^2 & -P_2 \cdot p_2 & -P_2 \cdot p_2^2 \\ \cdot & \cdot & \cdot & \cdot & \cdot \\ \cdot & \cdot & \cdot & \cdot & \cdot \\ 1 & p_n & p_n^2 & -P_n \cdot p_n & -P_n \cdot p_n^2 \end{bmatrix} \cdot \begin{bmatrix} c_0 \\ c_1 \\ c_2 \\ c_3 \\ c_4 \end{bmatrix} \quad (2)$$

$$L = A \cdot X \quad (3)$$

$$X = (A^t \cdot A)^{-1} \cdot A^t \cdot L$$

There are n observations in total. It can be said that the linking model is specified by determining the matrix X , according to Equation (3). By including the SO₂ emitted by the power plant in the proposed model, it is possible to calculate the projected pollutant concentration in nearby cities (Equation 4). The accuracy of the model fit based on Equation 5 is demonstrated by the difference between the calculated and monitored SO₂ values in surrounding cities.

$$\begin{bmatrix} P_1^a & 1 & p_1^a & p_1^{2a} & P_1^a \cdot p_1^a & P_1^a \cdot p_1^{2a} & c_0^a \\ P_2^a & 1 & p_2^a & p_2^{2a} & P_2^a \cdot p_2^a & P_2^a \cdot p_2^{2a} & c_1^a \\ \cdot & \cdot & \cdot & \cdot & \cdot & \cdot & c_2^a \\ \cdot & \cdot & \cdot & \cdot & \cdot & \cdot & c_3^a \\ P_n^a & 1 & p_n^a & p_n^{2a} & P_n^a \cdot p_n^a & P_n^a \cdot p_n^{2a} & c_4^a \end{bmatrix} \quad (4)$$

$$L' = A' \cdot X$$

P' and p' are the SO₂ concentrations in neighboring cities and the SO₂ emitted in TPP by the suggested model, respectively, in Equation (4).

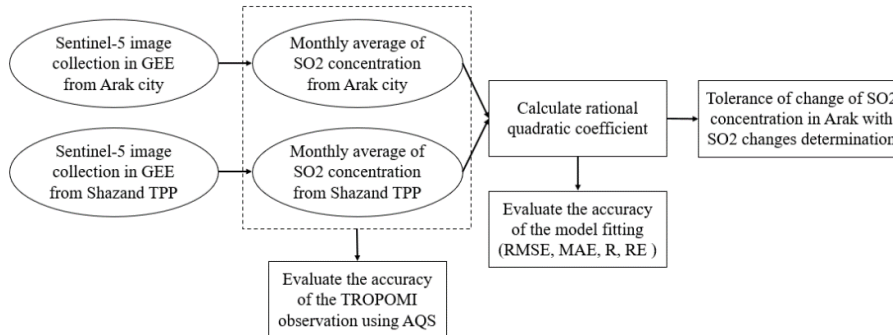


Figure 2. Flowchart of the proposed method

$$dL = L - L' = \begin{bmatrix} P_1 \\ P_2 \\ \cdot \\ \cdot \\ P_n \end{bmatrix} - \begin{bmatrix} P'_1 \\ P'_2 \\ \cdot \\ \cdot \\ P'_n \end{bmatrix} \quad (5)$$

dL is the model error matrix estimated in Equation (5). The smaller the dL , the better the proposed model can establish the relationship between the SO₂ produced in the TPP and the SO₂ concentration in the surrounding area.

Model fit and reliability were assessed using statistical measures of Root Mean Square Error (RMSE), Mean Absolute Error (MAE), Pearson's Correlation Coefficient. The relative error (RE) has also been used to evaluate the accuracy of the model fitting, as well as the model's validation and ability to estimate the values of the variable in other spatial locations. (Virghileanu et al., 2020) (Equation 6-9).

$$RMSE = \sqrt{\frac{\sum_{i=1}^n (L_i - L'_i)^2}{n}} \quad (6)$$

$$MAE = \frac{\sum_{i=1}^n |L_i - L'_i|}{n} \quad (7)$$

$$R = \frac{Cov(L, L')}{Var(L).Var(L')} \quad (8)$$

$$RE = \frac{RMSE}{\frac{\sum_{i=1}^n L_i}{n}} \quad (9)$$

3. Results and discussion

As already mentioned, the study area is Arak city and the Shazand TPP. Before explaining the implementation results of the proposed model, it is desirable to show Figure 3.

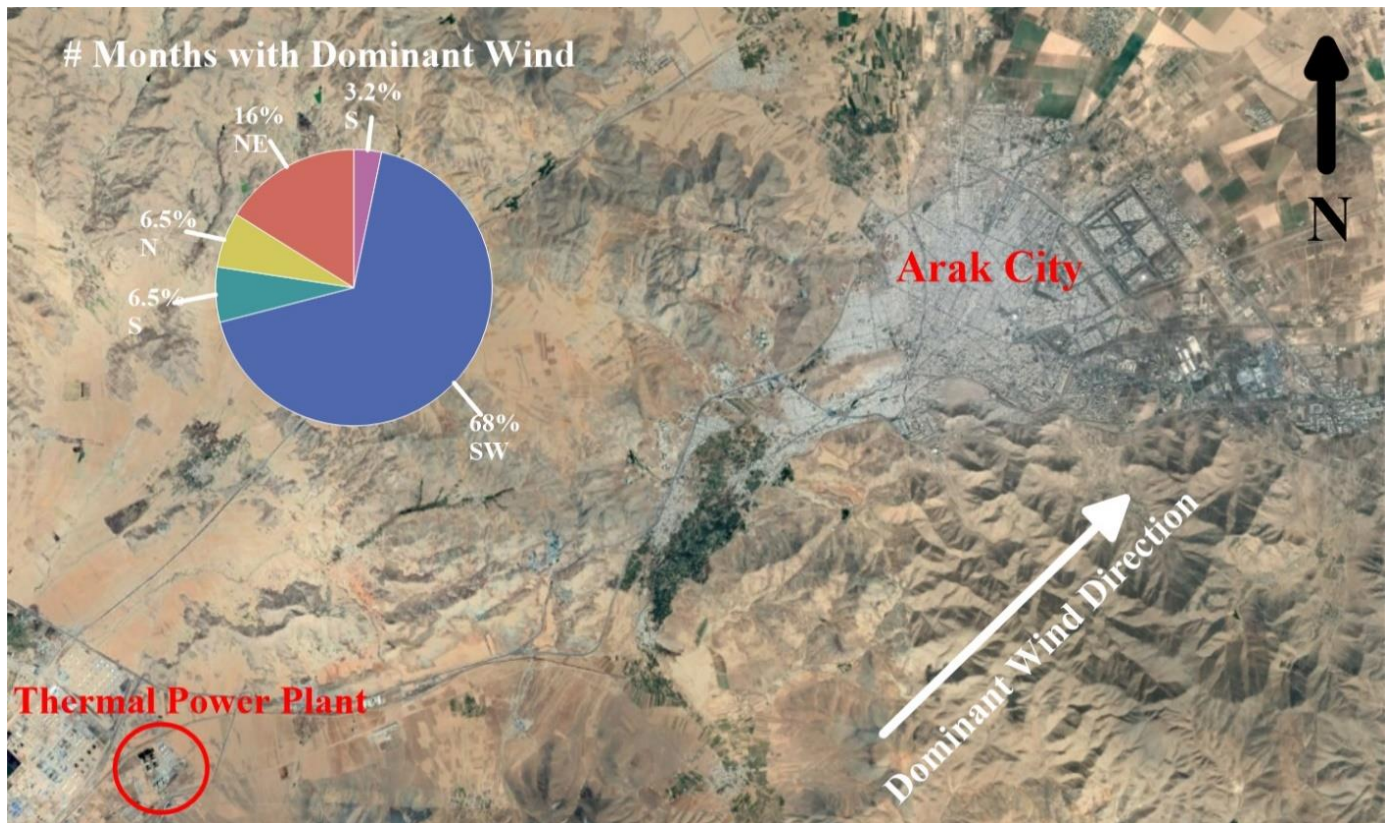


Figure 3. Location of Shazand TPP and Arak city along with the Dominant wind

As shown in Figure3, the monthly predominant wind blows from the southwest for 68% of the research period. This means that most of the pollutants emitted from the Shazand TPP end up in Arak. Considering that there are two mountain ranges in the region, one in the north and the other in the south, the wind is forced to pass through Arak. The level of air pollution is partially determined by weather conditions. In addition to wind speed and direction, the temperature has a significant effect on pollutant concentrations. Figure 4 depicts the changes in wind speed and temperature in the study area.

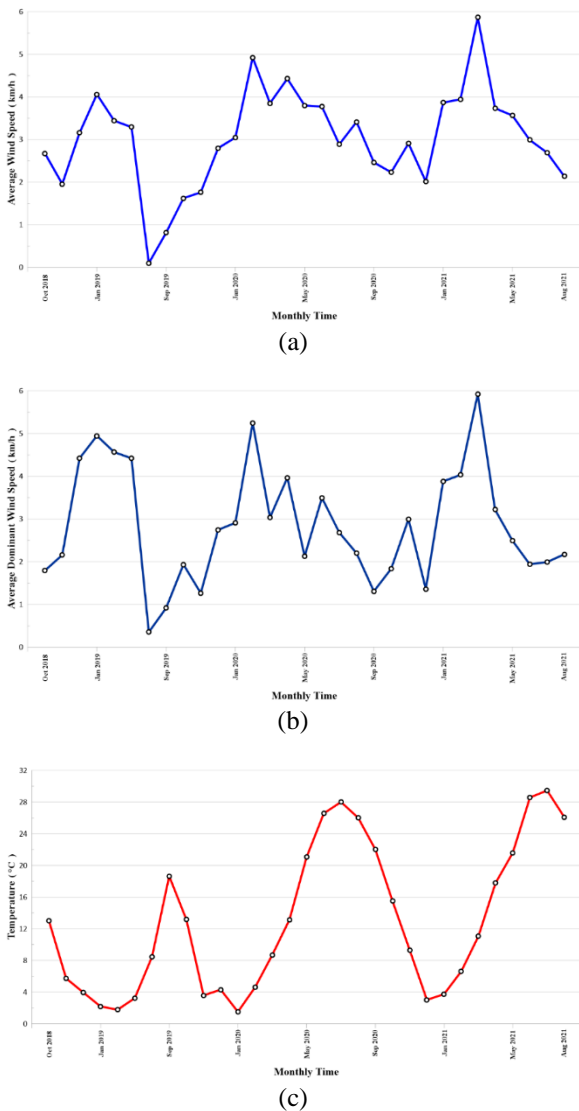


Figure 4. Changes in moderate (a) and dominant (b) wind speed and temperature (c) from Oct 2018 to Aug 2021

The coefficients of the proposed two-rational generic equation include the effects of wind, temperature, and other meteorological data.

Figure 5 shows the concentration of SO₂ emitted from Shazand TPP and the concentration of same pollutant in Arak, as measured by Sentinel-5 satellite Images. Comparing Figures 5 (a) and 5 (b), we can see the global pattern of changes in SO₂ concentration emitted from the Shazand TPP and SO₂ density in the city of Arak. Figure 6 shows the concentration of SO₂ pollutants emitted from the Shazand thermal power plant and the concentration of SO₂ in Arak. The cross-correlation between these observations is 0.73.

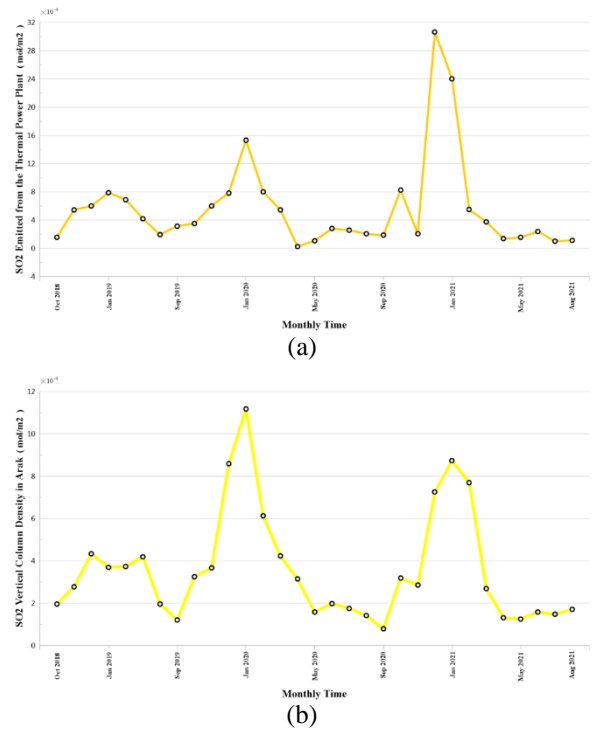


Figure 5. Observed SO₂ concentration by TROPOMI in Shazand TPP and Arak city from Oct 2018 to Aug 2021

The proposed Equation 1 is utilized to construct a relationship between the SO₂ concentration at the Shazand power plant and the concentration in Arak. The calculated SO₂ pollutant concentration values are compared with the observed values using the TROPOMI to evaluate the suitability of the proposed equation for the situation. As explained in the previous section, we evaluated the accuracy

using statistical metrics such as RMSE, MAE, relative error, and correlation coefficient. Figure 7 shows a comparison of these findings. Table 1 shows the criteria determined following comparison.

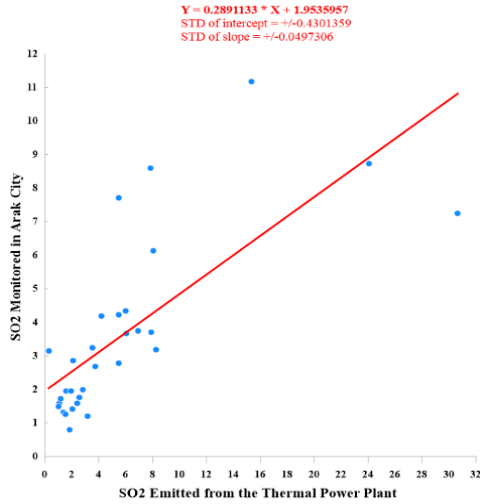


Figure 6. Comparison of SO2 vertical column density from TROPOMI emitted from Shazand TPP and observed in Arak city.

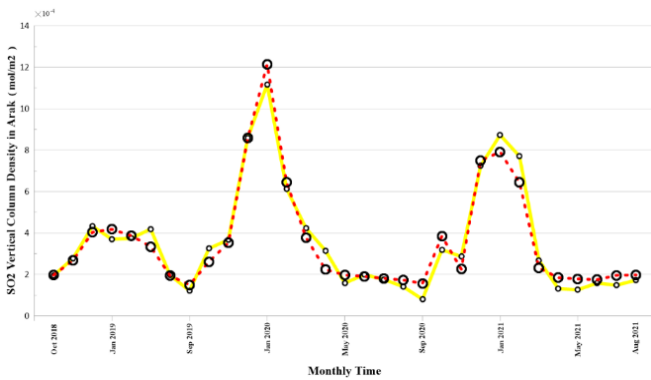


Figure 7. Comparison of computational SO2 concentration by the proposed equation (red line) with observable SO2 concentration by TROPOMI (yellow line) in Arak city

Table 1 Differences in SO2 concentrations were monitored and calculated using the proposed equation in the Arak city

RMSE	MAE	Relative Error	Correlation
0.54	0.42	0.15	0.98

The proposed equation is properly-suited to the situation, as shown in Table 1 and Figure 7.

In another experiment, by reducing and adding a certain amount (half of the standard deviation by the operator) to the concentration of SO2 emitted values in the Shazand power plant, the effects on the concentration of this pollutant have been investigated using the proposed equation in our study area. Figure 8 depicts these tolerances.

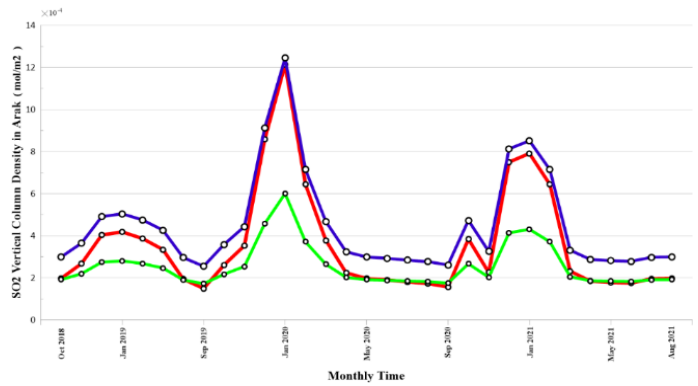


Figure 8. Tolerance of SO2 concentration changes in Arak with changes in SO2 released in the Shazand TPP based on proposed equation (Eq. 1)

As shown in Figure 8, monthly fluctuations in SO2 concentrations emitted from Shazand TPP can affect the concentration of this pollutant in the study area by 8 to 62 percent.

Table 2. shows the pollutant concentrations of SO2 in 2020 based on AQS (index) and TROPOMI (mol/m² × 10⁴) satellite measurements.

Month	Jan	Feb	Mar	Apr	May	Jun	Jul	Aug	Sep	Oct	Nov	Dec
AQS index	82	92	59.3	39.5	41.2	57.2	34.8	35	41.5	72.5	52.6	67.8
TROPOMI	11.17	6.13	4.23	3.15	1.58	1.99	1.76	1.41	0.8	3.19	2.86	7.25

The accuracy of Sentinel-5 observations is often assessed using ground-based AQS (Ialongo et al., 2020; Verhoelst et al., 2021). In addition, the accuracy of Sentinel-5 observations was assessed using the Arak AQS index. Monthly, we compared 2020 ground station observations with TROPOMI observations over the same period. Table 2 shows the outcomes of this comparison.

The cross-correlation coefficient between ground and satellite measurements was determined using the values in Table 2. The cross-correlation coefficient between Arak AQS and TROPOMI observations is acceptable at 0.77, indicating that Sentinel-5 data are reliable.

4. Conclusion

Air pollution is currently regarded as one of the most pressing challenges in Iran and the world, as it has a significant influence on climate change and human health. Toxic pollutants in the atmosphere, such as SO₂ harm human health. The sulfur component of fossil fuels produced by burning is the primary anthropogenic source of SO₂ emissions. The world's largest producer of SO₂ is a coal-fired power plant, which causes health problems such as pollution, acid rain, lung and respiratory illnesses. As an industrial city in Iran, Arak metropolitan area is constantly exposed to such pollutants, and the Shazand power plant is one of the largest producers of SO₂. Limited studies have

investigated the role of thermal power plants in air pollution in neighboring cities using satellite remote sensing. The Sentinel-5 satellite image used to collect SO₂ pollutant data in this study area can be considered as one of the most powerful tools for large-scale pollution monitoring. The subject of this research is the city of Arak. Arak is the capital of Markazi Province and one of the largest cities in Iran. Shazand is one of the most important industrial centers near Arak (TPP). SO₂, which is arguably the most important cause of burning fuel oil in the Shazand power plant and refinery, is one of the most hazardous pollutants in Arak. In this study, a three-year TROPOMI sensor image was used to propose a model of the relationship between SO₂ emitted by Shazand TPP and the amount of this pollutant in Arak a quadratic rational equation was applied to this relationship.

The main advantages of using these equations are flexibility and simplicity. The fitting accuracy (RMSE) of this equation was calculated to be 0.54. It has been discovered that adjusting the amount of SO₂ produced from TPP influences the level of this pollutant in Arak. This variation ranges from 8% to 62%. The Shazand power plant is oriented in the direction of the region's prevailing wind, and much of the pollutants emitted are transported to Arak. The final question is, why this has not been thoroughly investigated in the area where the Shazand thermal power plant has been built?

References

- Broomandi, P., Karaca, F., Nikfal, A., Jahanbakhshi, A., Tamjidi, M., & Kim, J. R. (2020). "Impact of COVID-19 event on the air quality in Iran." *Aerosol and Air Quality Research*, **20**(8), 1793-1804.
- Chen, C.-W., Tseng, Y.-S., Mukundan, A., & Wang, H.-C. (2021). "Air Pollution: Sensitive Detection of PM_{2.5} and PM₁₀ Concentration Using Hyperspectral Imaging." *Applied Sciences*, **11**(10), 4543.
- Chen, G., Li, S., Knibbs, L. D., Hamm, N. A., Cao, W., Li, T., . . . Guo, Y. (2018). "A machine learning method to estimate PM_{2.5} concentrations across China with remote sensing, meteorological and land use information." *Science of The Total Environment*, **636**, 52-60.
- de Vries, J., Voors, R., Ording, B., Dingjan, J., Veeffkind, P., Ludewig, A., ... & Aben, I. (2016, August). "TROPOMI on ESA's Sentinel 5p ready for launch and use. In Fourth international conference on remote sensing and geoinformation of the environment" (RSCy2016) (Vol. **9688**, p. 96880B). International Society for Optics and Photonics.
- Filippini, T., Rothman, K. J., Goffi, A., Ferrari, F., Maffei, G., Orsini, N., & Vinceti, M. (2020). "Satellite detected tropospheric nitrogen dioxide and spread of SARS-CoV-2 infection in Northern Italy." *Science of The Total Environment*, **739**, 140278.
- Ghasempour, F., Sekertekin, A., & Kutoglu, S. H. (2021). "Google Earth Engine based spatio-temporal analysis of air pollutants before and during the first wave COVID-19 outbreak over Turkey via remote sensing." *Journal of Cleaner Production*, **319**, 128599.

- Greenberg, N., Carel, R. S., Derazne, E., Bibi, H., Shpriz, M., Tzur, D., & Portnov, B. A. (2016). "Different effects of long-term exposures to SO₂ and NO₂ air pollutants on asthma severity in young adults." *Journal of toxicology and environmental health, Part A*, **79**(8), 342-351.
- Hedelt, P., Efremenko, D. S., Loyola, D. G., Spurr, R., & Clarisse, L. (2019). "Sulfur dioxide layer height retrieval from Sentinel-5 Precursor/TROPOMI using FP_ILM." *Atmospheric Measurement Techniques*, **12**(10).
- Ialongo, I., Virta, H., Eskes, H., Hovila, J., & Douros, J. (2020). "Comparison of TROPOMI/Sentinel-5 Precursor NO₂ observations with ground-based measurements in Helsinki." *Atmospheric Measurement Techniques*, **13**(1), 205-218.
- Kayes, I., Shahriar, S. A., Hasan, K., Akhter, M., Kabir, M., & Salam, M. (2019). "The relationships between meteorological parameters and air pollutants in an urban environment." *Global Journal of Environmental Science and Management*, **5**(3), 265-278.
- Koukouli, M.-E., Skoulidou, I., Karavias, A., Parcharidis, I., Balis, D., Manders, A., . . . van Geffen, J. (2021). "Sudden changes in nitrogen dioxide emissions over Greece due to lockdown after the outbreak of COVID-19." *Atmospheric Chemistry and Physics*, **21**(3), 1759-1774.
- Lelieveld, J., Evans, J. S., Fnais, M., Giannadaki, D., & Pozzer, A. (2015). "The contribution of outdoor air pollution sources to premature mortality on a global scale." *Nature*, **525**(7569), 367-371.
- Li, R., Wang, Z., Cui, L., Fu, H., Zhang, L., Kong, L., . . . Chen, J. (2019). "Air pollution characteristics in China during 2015–2016: Spatiotemporal variations and key meteorological factors." *Science of The Total Environment*, **648**, 902-915.
- Li, W., Thomas, R., El-Askary, H., Piechota, T., Struppa, D., & Ghaffar, K. A. A. (2020). "Investigating the significance of aerosols in determining the coronavirus fatality rate among three European Countries." *Earth Systems and Environment*, **4**(3), 513-522.
- Lin, C., Li, Y., Yuan, Z., Lau, A. K., Li, C., & Fung, J. C. (2015). "Using satellite remote sensing data to estimate the high-resolution distribution of ground-level PM 2.5." *Remote Sensing of Environment*, **156**, 117-128.
- Lorente, A., Borsdorff, T., Butz, A., Hasekamp, O., Schneider, A., Wu, L., . . . Pollard, D. F. (2021). "Methane retrieved from TROPOMI: improvement of the data product and validation of the first 2 years of measurements." *Atmospheric Measurement Techniques*, **14**(1), 665-684.
- Omrani, H., Omrani, B., Parmentier, B., & Helbich, M. (2020). "Spatio-temporal data on the air pollutant nitrogen dioxide derived from Sentinel satellite for France." *Data in brief*, **28**, 105089.
- Quesada-Ruiz, S., Attié, J.-L., Lahoz, W. A., Abida, R., Ricaud, P., Amraoui, L. E., . . . Eskes, H. (2020). "Benefit of ozone observations from Sentinel-5P and future Sentinel-4 missions on tropospheric composition." *Atmospheric Measurement Techniques*, **13**(1), 131-152.
- Safarianzengir, V., Sobhani, B., Yazdani, M. H., & Kianian, M. (2020). "Monitoring, analysis and spatial and temporal zoning of air pollution (carbon monoxide) using Sentinel-5 satellite data for health management in Iran, located in the Middle East." *Air Quality Atmosphere and Health*.
- Saxena, P., & Naik, V. (2018). "Air pollution: sources, impacts and controls" CABI.
- Schneising, O., Buchwitz, M., Reuter, M., Bovensmann, H., Burrows, J. P., Borsdorff, T., . . . Hase, F. (2019). "A scientific algorithm to simultaneously retrieve carbon monoxide and methane from TROPOMI onboard Sentinel-5 Precursor." *Atmospheric Measurement Techniques*, **12**(12), 6771-6802.
- Shikwambana, L., Mhangara, P., & Mbatha, N. (2020). "Trend analysis and first time observations of sulphur dioxide and nitrogen dioxide in South Africa using TROPOMI/Sentinel-5 P data." *International Journal of Applied Earth Observation and Geoinformation*, **91**, 102130.
- Sohn, H. G., Park, C. H., & Chang, H. (2005). "Rational function model - based image matching for digital elevation models." *The Photogrammetric Record*, **20**(112), 366-383.
- Sun, W., Zhu, L., De Smedt, I., Bai, B., Pu, D., Chen, Y., . . . Wang, X. (2021). "Global significant changes in formaldehyde (HCHO) columns observed from space at the early stage of the COVID - 19 pandemic." *Geophysical Research Letters*, **48**(4), 2e020GL091265.
- Tang, L., Xue, X., Qu, J., Mi, Z., Bo, X., Chang, X., . . . Dong, G. (2020). "Air pollution emissions from

- Chinese power plants based on the continuous emission monitoring systems network." *Scientific Data*, **7**(1), 1-10.
- Theys, N., Hedelt, P., De Smedt, I., Lerot, C., Yu, H., Vlietinck, J., . . . Fernandez, D. (2019). "Global monitoring of volcanic SO₂ degassing with unprecedented resolution from TROPOMI onboard Sentinel-5 Precursor." *Scientific reports*, **9**(1), 1-10.
- Tiwari, S., Srivastava, A., Singh, A., & Singh, S. (2015). "Identification of aerosol types over Indo-Gangetic Basin: implications to optical properties and associated radiative forcing." *Environmental Science and Pollution Research*, **22**(16), 12246-12260.
- Verhoelst, T., Compernelle, S., Pinardi, G., Lambert, J.-C., Eskes, H. J., Eichmann, K.-U., . . . Cede, A. (2021). "Ground-based validation of the Copernicus Sentinel-5p TROPOMI NO₂ measurements with the NDACC ZSL-DOAS, MAX-DOAS and Pandora global networks." *Atmospheric Measurement Techniques*, **14**(1), 481-510.
- Vigouroux, C., Langerock, B., Bauer Aquino, C. A., Blumenstock, T., Cheng, Z., De Mazière, M., . . . Jones, N. (2020). "TROPOMI-Sentinel-5 Precursor formaldehyde validation using an extensive network of ground-based Fourier-transform infrared stations." *Atmospheric Measurement Techniques*, **13**(7), 3751-3767.
- Virghileanu, M., Săvulescu, I., Mihai, B.-A., Nistor, C., & Dobre, R. (2020). "Nitrogen Dioxide (NO₂) Pollution Monitoring with Sentinel-5P Satellite Imagery over Europe during the Coronavirus Pandemic Outbreak." *Remote Sensing*, **12**(21), 3575.
- Wang, G., Deng, J., Zhang, Y., Zhang, Q., Duan, L., Hao, J., & Jiang, J. (2020). "Air pollutant emissions from coal-fired power plants in China over the past two decades." *Science of The Total Environment*, **741**, 140326.
- Wang, L., Li, M., Yu, S., Chen, X., Li, Z., Zhang, Y., . . . Liu, W. (2020). "Unexpected rise of ozone in urban and rural areas, and sulfur dioxide in rural areas during the coronavirus city lockdown in Hangzhou, China: implications for air quality." *Environmental Chemistry Letters*, **18**(5), 1713-1723.
- Zeng, S., & Zhang, Y. (2017). "The Effect of Meteorological Elements on Continuing Heavy Air Pollution: A Case Study in the Chengdu Area during the 2014 Spring Festival." *Atmosphere*, **8**(4), 71.
- Zhang, Y. (2019). "Dynamic effect analysis of meteorological conditions on air pollution: A case study from Beijing." *Science of The Total Environment*, **684**, 178-185.
- Zhao, F., Liu, C., Cai, Z., Liu, X., Bak, J., Kim, J., . . . Sun, Y. (2021). "Ozone profile retrievals from TROPOMI: Implication for the variation of tropospheric ozone during the outbreak of COVID-19 in China." *Science of The Total Environment*, **764**, 142886.